



ELSEVIER

Contents lists available at ScienceDirect

Ad Hoc Networks

journal homepage: www.elsevier.com/locate/adhoc

Coverage and connectivity in three-dimensional networks with random node deployment

S.M. Nazrul Alam^a, Zygmunt J. Haas^{b,*}^a Google Inc., Mountain View, CA, USA^b School of Electrical and Computer Engineering, Cornell University, Ithaca, NY, USA

ARTICLE INFO

Article history:

Received 5 March 2014

Received in revised form 12 August 2014

Accepted 13 September 2014

Available online xxxx

Keywords:

Three-dimensional networks

3D networks

Coverage and connectivity

Polyhedron

Node placement

 k -Coverage

ABSTRACT

The increasing interest in using sensor networks in applications for underwater surveillance and oceanic studies underscores the importance of solving the coverage and connectivity issues in 3D wireless sensor networks (WSN). In particular, the problem of supporting full coverage, while ensuring full network connectivity is a fundamental one for such applications. Unfortunately, designing a 3D network is significantly more difficult, as compared to designing a 2D network. Previously, it has been shown that dividing a 3D space into identical truncated octahedral cells of radius equal to the sensing range and placing a sensor at the center of each cell, provides full coverage with minimum number of nodes [2]. But this requires the ability to deploy and maintain sensor nodes at such particular locations. In many environments, this is very difficult, if not impossible, to do. In this paper, we investigate the coverage and connectivity issues for such 3D networks, especially underwater networks, while assuming random and uncontrollable node locations. Since node location can be random, redundant nodes have to be deployed to achieve 100% sensing coverage. However, at any particular time, not all nodes are needed to achieve full sensing coverage. As a result, a subset of the nodes can be dynamically chosen to remain active at a time to achieve sensing coverage based on their location at that time. One approach to achieve this goal in a distributed and scalable way is to partition the 3D network volume into virtual regions or cells, and to keep one node active in each cell. Our results indicate that using cells created by *truncated octahedral tessellation* of 3D volume minimizes the number of active nodes. This scheme is fully distributed, and so it is highly scalable. By adjusting the radius of each cell, this scheme can be used to achieve k -coverage, where every point inside a network has to be within the sensing range of k different sensor nodes. We analyze and compare the performance of these schemes for both 2D and 3D networks. While for 1-coverage, the 3D scheme is less efficient than the 2D scheme, the performance of 3D scheme improves significantly as compared to 2D scheme for k -coverage, for values of k is larger than 1. As a result, such a distributed and scalable scheme can be more useful in 3D networks than in 2D networks. Although this paper targets in particular 3D underwater networks, much of our results are applicable to other 3D networks, such as for airborne applications, space exploration, and storm tracking.

© 2014 Elsevier B.V. All rights reserved.

1. Introduction

Applications of sensor networks for underwater applications such as exploitation, surveillance, oceanic

* Corresponding author.

E-mail addresses: smnalam@google.com (S.M. Nazrul Alam), haas@ece.cornell.edu (Z.J. Haas).<http://dx.doi.org/10.1016/j.adhoc.2014.09.008>

1570-8705/© 2014 Elsevier B.V. All rights reserved.

study, (as well as in other applications such as space exploitation, airborne surveillance and greenhouse gas monitoring) require deployment of 3D wireless sensor networks. Although practical wide-scale deployment of 3D networks is still relatively limited, there has much work in progress that promises to make 3D networks significantly more ubiquitous in the not-so-far future. For example, underwater acoustic sensor networks have generated a lot of interest among researchers [1,11,15,19,38–41,43]. Ocean column monitoring requires the nodes to be placed at different depths of ocean, which creates a three-dimensional network [1]. In an article of Business 2.0 magazine, eight technologies have been identified that can save the world from global warming and its catastrophic consequences [13]. That article identifies environmental sensor networks as one of those eight technologies. Since sensor nodes in such environmental wireless sensor networks will be distributed over a 3D space, they must be modeled as a 3D network as well.

Many detection and tracking applications require full coverage such that any point inside the network volume (also referred to here as network space) is monitored at any time by at least one sensor [5,9,12,23,25,33]. It is also important to maintain connectivity, so that detection information can be transmitted to the sink or a command center. While coverage and connectivity issues have been thoroughly investigated in the technical literature, the scope of most of those works relates to terrestrial 2D sensor networks. Unfortunately, many of those results cannot be directly applied to 3D networks. In fact, many widely used coverage analysis and placement strategies developed for 2D networks become NP-Hard in 3D [36]. It is not surprising, given the historical fact that many problems in 3D required many centuries of effort to be solved, while their 2D counterparts can be solved trivially. For example, Kepler's sphere packing problem has been around since 1611, but a proof of Kepler's conjecture has only been found in 1998 [17]. It is still an open problem if Kelvin's conjecture holds when the cells have identical shape. Similarity with Kelvin's conjecture has been used before to solve coverage and connectivity problem in 3D networks [2,3]. But these works are applicable only under the assumption that sensor nodes can be deployed and maintained at specified arbitrary locations. Although this assumption may be realistic in some communication environments, it could be considered less practical in large deployment of underwater sensor networks. In this paper, we investigate the coverage and connectivity issues in 3D networks where this latter assumption does not hold. Instead, we assume that we have no control over the movement of a node. As a result, the position of a node can be random and a large number of redundant nodes have to be deployed in order to ensure that every point of the network is within the sensing range of at least one sensor node. However, at any time instant usually not all nodes are needed for full sensing coverage. The challenge is to find a distributed and scalable scheme that dynamically selects a suitable subset of nodes to remain active based on their location, while putting other nodes into sleep mode. Since energy consumption during sleep mode is insignificant, this approach prolongs network lifetime significantly. Although it is possible to solve this problem

in many different ways, however, finding a distributed and scalable scheme that adjusts in real-time with changes in the network topology (e.g., movement of nodes) is difficult [28]. Any solution that depends on a lot of message passing is unlikely to achieve this objective, especially because of the particular characteristics of the underwater communication environment.

In this paper, we propose a very fast, distributed, and scalable scheme to dynamically select a subset of active nodes, such that full sensing coverage and connectivity is always maintained. We assume that sensing and communication range of each sensor node is deterministic, homogeneous, and spherical. It is also assumed that each sensor node has a localization component that allows it to determine its position. (Such schemes have been studied extensively in the technical literature; see e.g., [44–46].) The main idea is to divide the 3D network space into identical regions based on the sensing range and communication range of the sensor nodes. Among the sensor nodes located in each region, one sensor node is dynamically and locally selected to perform the sensing operation for that region and to maintain connectivity with active nodes of the neighboring regions.

Although this general idea has been used before [34], the challenging part is to determine the best possible division that minimizes the number of regions (and thus minimizes the number of active nodes at any time). There are two constraints here. First, the diameter of the circumsphere of each region cannot be greater than the sensing range of each sensor node. This is because, unlike in [2,3], we do not have any control of the position of the node. In the extreme case, it is possible that the selected active node is located in one corner of the region. Still this sensor node must be able to sense all the points of its region. Second, maximum distance between two furthest points of the neighboring regions cannot be greater than the communication range of each sensor node. This constraint guarantees that active nodes of two neighboring region are able to communicate between them, irrespective of their positions inside each region. These two constraints ensure that full coverage and connectivity are maintained even though active nodes are selected locally by the nodes inside each region.

Our contributions, results, and conclusions of this work can be summarized as follows:

- We investigate the problem of coverage and connectivity for 3D networks where deployment of a node at any predetermined position and maintaining that node position cannot be ensured. As a result, a large number of nodes have to be randomly deployed. Since at any particular time, all nodes are not needed for maintaining full sensing coverage and connectivity, it is important to put the redundant nodes into sleep mode, thus limiting the energy use and prolongs the network lifetime. This must be done in a dynamic fashion based on the position of the nodes at that instant. The scheme must be highly distributed and scalable, because node movement is unpredictable. We introduce such a scheme that dynamically determines the active node locally.

- Our scheme partitions the 3D network space into regions (or, cells) and keeps one node active in each cell. Partitioning must be done in such a way that the number of cells is minimal (again, to prolong the network lifetime), while ensuring that the active node, which can be located anywhere inside the cell, can monitor the entire cell and that the active node is able to communicate with active nodes of all the neighboring cells. Using Kelvin's conjecture, we speculate that this can be achieved if the shape of the cell is *truncated octahedral*. We define a metric called *volumetric quotient* ($V.Q.$) which is the ratio of the volume of a polyhedron to the volume of its circumsphere. The larger the $V.Q.$ of the shape of cell is, the smaller is the number of the required active nodes. We show that the $V.Q.$ of truncated octahedron is 0.68329, much larger than other possible space-filling polyhedrons. For example, the $V.Q.$ of *rhombic dodecahedron* is 0.477, *hexagonal prism* has volumetric quotient of 0.477, and *cube* has just 0.36755. These results imply that if the shape of the cell is rhombic dodecahedron or hexagonal prism, then we need 43.25% more nodes than in the case when the shape of the cell is truncated octahedron. We also compare different partitioning scheme based on their energy efficiency. We find that cell lifetime is maximized if we use truncated octahedron based cell.
- We provide a very simple mechanism that allows each sensor node to identify their cell id instantly if they know their own position. This scheme requires only a constant number of arithmetic operations to compute the cell id of each node and hence is computationally very efficient. Once they identify their cell id, the sensor nodes can easily choose the active node locally.
- While our scheme is highly distributed and scalable, and active nodes are dynamically selected locally in each cell without any message passing between nodes in different cells, sometime the scheme keeps more nodes active than a centralized scheme that has global knowledge about the position of all nodes. We compare the efficiency of our scheme with that of a centralized scheme that can deploy nodes at any arbitrary location. Since such a centralized scheme can control the position of the nodes, it requires even fewer active nodes than the optimal scheme that cannot control the position of the nodes. In order to highlight this distinction, we call this centralized scheme *SuperOpt*. We compare our scheme with *SuperOpt* for k -coverage, where a point is monitored by k sensor nodes rather than just one sensor node. We found that the gap between our scheme and *SuperOpt* decreases significantly when k is greater than 1. While the ratio of the number of active nodes between the distributed scheme and *SuperOpt* goes down both in 2D and 3D, only in 3D k -coverage can be maintained with high probability.

The rest of the paper is organized as follows. Section 2 presents some necessary background information on space-filling polyhedron, Voronoi tessellation, famous conjectures of Kelvin and Kepler, and describes related works in network literature. Section 3 formally describes the problem and the assumptions. Section 4 analyzes the

problem and describes the results. Section 5 discusses how our scheme can be adjusted when the ideal assumptions are not valid. Finally, Section 6 concludes the paper.

2. Preliminaries

In this section, we define some relevant terms and provide some background information necessary for the presentation of our research. The last subsection describes selected related works in the technical literature.

2.1. Space-filling polyhedron

A *polyhedron* is a three-dimensional shape consisting of finite number of polygonal faces. The faces meet in straight line segments called *edges* and the edges meet at points called *vertices* of the polyhedron. A polyhedron surrounds a bounded volume in three-dimension. Example of polyhedrons includes *cubes*, *prisms*, and *pyramids*. *Polygon* is a two-dimensional analog of polyhedrons. The general term for a shape of any dimension is *polytope*.

A *space-filling polyhedron* is a polyhedron that can be used to perfectly fill a volume of space, without overlaps or gaps (a.k.a. tessellation or tiling). At first, we provide a short overview on space-filling polyhedron. It is not easy to show that a polyhedron has space-filling property. For example, although Aristotle claimed that the tetrahedron fills space [4], his claim was incorrect [18], and the mistake remained unnoticed until the 16th century [22].

Some of the important results on space-filling polyhedron are as follows: There are exactly five regular polyhedrons (a.k.a. platonic solids or regular solids) [26]: *cube*, *dodecahedron*, *icosahedron*, *octahedron*, and *tetrahedron*, as was proved by Euclid in the last proposition of the *Elements* ([42]). Among them, only cube has the space-filling property [16]. There are only five convex polyhedrons with regular faces having space-filling property: *triangular prism*, *hexagonal prism*, *cube*, *truncated octahedron* [26,31], and *gyrobifastigium* [20]. The *rhombic dodecahedron*, *elongated dodecahedron*, and *squashed dodecahedron* are also space-fillers. A combination of tetrahedrons and octahedrons fills space. In addition, octahedrons, truncated octahedrons, and cubes, combined in the ratio 1:1:3, can also fill space.

2.2. Kelvin's conjecture

In 1887, Lord Kelvin asked the following question [27]: "What is the optimal way to fill a three dimensional space with cells of equal volume so that the surface area (interface area) is minimized?" This is essentially a problem of finding a space-filling structure having the highest *isoperimetric quotient*. If the volume and surface area of a structure are V and S , respectively, then in three-dimensions its isoperimetric quotient can be defined as $\frac{36\pi V^2}{S^3}$. Sphere has the highest isoperimetric quotient and it is 1. Kelvin's answer for his question was 14-sided truncated octahedron having a very slight curvature of the hexagonal faces and its isoperimetric quotient is 0.757, but he could not prove that it is optimal. Uncurved truncated octahedron has isoperimetric quotient of 0.753367. For more than a century,

Kelvin's solution was generally accepted as correct [32] and is widely known as *Kelvin's conjecture*. But in 1994, two physicists Denis Weaire and Robert Phelan came up with another space-filling structure consisting of six 14-sided polyhedrons and two 12-sided polyhedrons with irregular faces of equal volume that has 0.3% less surface area than truncated octahedron [29,30]. The isoperimetric quotient of this structure is 0.764. But any proof that the structure of Weaire and Phelan is optimal, or that Kelvin's solution is optimal for identical cells, is yet to be found.

2.3. Voronoi tessellation

In three-dimension, for any (topologically) discrete set S of points in Euclidean space, the set of all points closer to a point c of S than to any other point of S is the interior of a convex polyhedron called the *Voronoi cell* for the point c (see e.g., [6]). The set of such polyhedrons tessellate the whole space, and is called the *Voronoi tessellation* corresponding to the set S . If we find the solution of our problem, i.e., the optimal location of the nodes, then their Voronoi tessellation provides the optimal shape of each cell.

2.4. Kepler's conjecture

Another closely related problem is Kepler's sphere packing problem. The problem is to find the most efficient way to pack a volume using equal-sized spheres. In 1611, Kepler made a guess that the face-centered cubic (FCC) lattice was the most efficient of all arrangements, but was unable to prove this. After four hundred years of failed efforts, Kepler's conjecture was finally proved to be correct by Thomas Hales in 1998 [10]. The proof extensively uses methods from the theory of global optimization, linear programming, and interval arithmetic. The computer code and data files used for the proof required more than 3 GB of space for storage. The Voronoi tessellation of face-centered cubic (FCC) lattice is rhombic dodecahedron and although FCC lattice is the optimal solution for sphere packing, in this paper we will show that truncated octahedron, which is the Voronoi tessellation of body-centered cubic (BCC) lattice, actually require 43.25% fewer nodes for our problem. This significant difference is not very intuitive. Note that, FCC lattice has packing density of 74.048% (optimal solution for sphere packing) while BCC lattice has packing density of about 68%.

2.5. Related works in networks

Conserving energy, and thus prolonging the network lifetime, by keeping a subset of the nodes active in a dense network while putting the rest of the nodes into sleep mode has been proposed for terrestrial 2D sensor networks [7,10,34,35,37]. Some of these works can be applied to 3D networks as well. Our work in this paper is most closely related to geographic adaptive fidelity (GAF) [34], while extending its scope. However [34] is only applicable to 2D networks and extending that work to 3D network is very difficult, because it is hard to find best partitioning scheme in 3D. We investigate this problem in our paper. Another limitation of GAF is that sometime it requires

more nodes than a centralized scheme with global information about node locations. We address that issue by providing an innovative scheme for k -coverage. Our scheme achieves k -coverage with high probability, while significantly decreasing the gap in the number of active nodes needed relative to the centralized scheme.

As selected examples only, we mention here a few other references on three-dimensional networks in the literature. Modeling 3D cellular networks has been investigated in [8,14]. Shape of the cell is modeled as rhombic dodecahedron in [8] and in [14] each cell is represented as hexagonal prism. However, our work shows that both rhombic dodecahedron and hexagonal prism shaped cell requires 43.25% more active nodes than the case when the shape of the cell is truncated octahedron. Coverage and connectivity issues of 3D networks have been investigated in [2,3]. However, those works assume that nodes can be deployed at any desired location and that the positions of those nodes can be maintained during the entire lifetime of the network. In this paper, we investigate the case where this assumption does not hold, which would be the practical case of underwater sensor nodes without being equipped with self-propelling means.

3. Problem statement

The main assumptions and the problem goals are defined as follows.

3.1. Assumptions

- Sphere-based sensing: We assume a sphere based sensing model such that each active sensor has a sensing range of r_s ; an active sensor can reliably detect any object that is located within a distance of r_s from the sensor.
- Sphere-based communication: We assume a spherical communication model where each active sensor has a transmission range (or, communication range) of r_t ; i.e., if the distance between two active sensors is less than or equal to r_t , then they can communicate reliably with each other.
- Homogeneous sensing and communication range: We assume that all sensors have the same sensing range and that the communication range of all sensors is also identical.
- No boundary effect: We assume that the network is very large and there is no boundary effect, so that the number of nodes required for a placement strategy is inversely proportional to the volume of a Voronoi cell of the nodes.
- Random node position: We make no assumption about the location where any particular node is deployed. However, sensor node density must be high enough, so that full coverage can be maintained.

3.2. Goal

The main goal is to find a distributed scalable scheme to dynamically determine the subset of nodes that remains

active. As shown in the next section, we accomplish this goal by achieving the following sub-goals.

- Given any fixed sensing range r_s , find the best partitioning scheme that keeps minimum number of required active nodes at any time. Also find out the best partitioning scheme such that lifetime of a cell (i.e., time until the last node in a cell dies out) is maximum.
- Find a distributed and efficient algorithm for the determination of which cell a sensor node belongs to.
- Find a solution for k -coverage problem, such that any point is within the sensing range of at least k nodes. Determine the efficiency of the scheme compared to an optimal scheme where an “oracle” determines which nodes to keep active and nodes position can be adjusted as needed.

4. Analysis

One simple distributed and scalable scheme to dynamically determine the subset of nodes that needs to remain in active mode is as follows. Partition the 3D network space into identical regions (i.e., cells) in such a way that if any node inside that region is active, it can monitor the entire region. Thus full sensing coverage can be achieved by locally selecting an active node in each such a cell. No coordination or message passing with nodes outside the cell is needed. Local selection of the active node can be done based on any standard leader selection algorithm¹ (e.g., [24]) and the leader can be selected to serve as the active node. All other nodes go into sleep mode until the leader dies or moves to another cell. In order to maintain connectivity among nodes, partitioning must be done in such a way that the distance between two active nodes from neighboring region must be less than or equal to the transmission range, r_t . This simple but powerful scheme does not require any coordination with nodes outside the cell and so is highly distributed and scalable. Furthermore, this scheme can also quickly adapt to rapid node movement. (The assumption here is that the topological changes resulting from nodes' movement is slower than the rate at which the active node selection is performed.) However, there are two main considerations that need to be addressed:

1. Node density must be large enough, so that there is at least one node in each cell to provide full sensing coverage.
2. In some cases, this scheme is less than optimal in terms of the number of active nodes. (Later in this paper, we investigate the requirement of the number of active nodes for k -coverage, where the goal is to provide monitoring by k sensor nodes of each location (instead of just one sensor node). We found that in 3D networks, relative requirement of the number of active nodes goes down for larger values of k , while the probability of k -coverage remains very large.)

¹ Leader selection can be as simple as choosing the node that is closest to the center of the cell. In the case of a tie, node energy level or node id can be used as a tie breaker.

While the scheme mentioned above is interesting and analog to a scheme that had been investigated in the context of 2D networks [34], one major and challenging problem is to find the right partitioning procedure in the context of 3D networks.

4.1. Determining the right partitioning scheme

In order to find the right partitioning scheme, it is important to identify the criteria of what constitute the best partitioning scheme. One criterion could be minimizing the number of active nodes at any instant. Since there is one active node per cell, minimizing the number of cells achieves this goal. In order to obtain a general solution, we assume that the 3D network volume to be monitored is infinite, so there are no boundary effects. Although, it may be the case that the best partitioning scheme does not create identical cells, we assume that all cells are identical for the following reasons:

1. This makes the problem tractable and allows us to focus on the shape of the cell.
2. Identical cells provide a regular pattern and allow us to deterministically establish the location of any cell using a simple set of equations. This is important to make the algorithm efficiently fully distributed and scalable.
3. Due to symmetry and infiniteness of the 3D network space, it is unlikely that the shape of cells will be different in the best partitioning scheme.
4. Practical deployment of the scheme in an underwater environment would be significantly simplified with the use of identical cells.

If the shape of all cells is identical, then maximizing the volume of a cell minimizes the number of cells. There are three following constraints:

1. Shape of a cell must be a space-filling polyhedron.
2. Diameter of the circumsphere of the cell cannot be greater than the sensing range, r_s .
3. Distance between two furthest points of two neighboring cells cannot be greater than the transmission range, r_t .

The first constraint limits the number of possible polyhedrons. Since maximizing the volume is the goal, for any shape of the cell, the diameter of the circumsphere must always be r_s . Thus the volume of the circumsphere must be: $\frac{4}{3}\pi(\frac{r_s}{2})^3 = \frac{\pi r_s^3}{6}$, which is the upper bound of the volume of the cell. This allows us to create an instinctively useful metric, defined as the ratio of the volume of a cell to the volume of its circumsphere, useful for comparing different shapes of a cell. We refer to this metric as *volumetric quotient* ($V.Q.$). If the volume of a cell is V , then, its $V.Q.$ is: $\frac{6V}{\pi r_s^3}$. The value of $V.Q.$ is always between 0 and 1. Our goal is to find the space-filling polyhedron with the largest (i.e., closest to 1) $V.Q.$

Finding the optimal polyhedron and proving its optimality seems to be a very hard problem, given that many of the 3D optimality problems them took centuries to

prove (Kelvin's problem is still open after more than one century, while Kepler's conjecture was proven only recently after almost five centuries of efforts). Since providing any rigorous proof is likely to be an intractable problem, we proceed in the following way. At first we provide some intuition why truncated octahedron is the most likely solution by drawing similarity of our problem with the Kelvin's conjecture. Then we choose three other different space-filling polyhedrons that have been used by other researchers in similar problems and are reasonable contenders to truncated octahedron as a possible solution. We then show that truncated octahedron has much higher $V.Q.$ than other contenders and, thus, requires much fewer active nodes.

Kelvin's problem is essentially finding a space-filling polyhedron that has minimum ratio of surface-area to volume. We claim that the space-filling polyhedron that has the minimum ratio of surface-area to volume should best approximate the sphere. It is well known that among all structures:

1. For a given volume, sphere has the smallest surface area.
2. For a given surface area, sphere has the largest volume.

From above two statements, we claim the following. Suppose that any two space-filling polyhedrons P_1 and P_2 have equal volume. If surface-area of P_1 is smaller than the surface area of P_2 , then P_1 is a better approximation of sphere than P_2 . Again if P_1 is a better approximation of sphere than P_2 , then P_1 has higher volumetric quotient than P_2 . Recall that among all shapes, sphere has the highest volumetric quotient, which equals to 1.

Thus the solution of the Kelvin's problem is essentially the solution of our problem. Since until now, truncated octahedron is the best known solution for Kelvin's problem for a single cell shape, we conjecture that truncated octahedron is also the most likely solution for our problem. Note that, we will consider the uncurved version of truncated octahedron, because it is mathematically more tractable than the curved version and the difference between the curved version and the uncurved version is practically negligibly small. Since the argument given above is not strictly rigorous, so next we choose other likely contenders of truncated octahedron and provide comparison of truncated octahedron with those space-filling polyhedrons.

One can attempt to solve our problem using Kepler's problem in the following way. Find the maximal packing of spheres and then select the Voronoi tessellation corresponding to the centers of the spheres. Define the radius of the spheres such that the maximum distance from a center to any vertex of the corresponding Voronoi cell is the sensing range, r_s . Kepler's conjecture for sphere packing problem has been proven recently after five centuries of efforts, with the Face-Centered Cubic (FCC) lattice being the solution for that problem. The Voronoi tessellation of FCC lattice is rhombic dodecahedron. So we choose rhombic dodecahedron as one of the contender of truncated octahedron.

As another attempt, consider the fact that the solution of our problem in 2D is hexagon [21]. The polyhedron that has hexagon as its cross section in all three directions (x , y , and z) does not have space-filling property. The polyhedrons that have space-filling property and hexagonal cross section are rhombic dodecahedron and hexagonal prism. So, we include both in our comparison. Finally, most simplistic choice is cube and it is the only regular polyhedron that tessellates in 3D space. So we compare truncated octahedron with rhombic dodecahedron, hexagonal prism, and cube, and show that truncated octahedron has better volumetric quotient than the rest of the choices and hence required fewer nodes to cover a given volume.

Given the diameter of the circumsphere to be r_s , we determine that $V.Q.$ -s of cube, rhombic dodecahedron and truncated octahedron as: $\frac{2}{\sqrt{3}\pi} = 0.36755$, $\frac{3}{2\pi} = 0.477$, $\frac{24}{5\sqrt{5}\pi} = 0.68329$, respectively. In the case of hexagonal prism, diameter of the circumsphere does not ensure a unique hexagonal prism. This is because, there can be many hexagonal prisms with different heights and different sizes for the hexagonal faces and still have the same diameter for their circumsphere. We chose the hexagonal prism that has the highest $V.Q.$ and found it to be $\frac{3}{2\pi} = 0.477$. Clearly, if the truncated octahedron is the shape of the cell, then the number of active nodes is the fewest.

Next, we consider the arrangement of four types of cell. We call their regular 3D tessellation as CB (for cube), HP (for hexagonal prism), RD (for rhombic dodecahedron), and TO (for truncated octahedron) models. For cube and hexagonal prism, several alternate arrangements of cells are possible by shifting one layer with respect to another neighboring layer. We consider the furthest possible movement, where one corner of a cell is at the center of a cell in the neighboring layer, and call these models *Alt-CB* and *Alt-HP* (see Fig. 1). Considering only these two alternative arrangements (for both cube and hexagonal prism) is sufficient, as in each cases they are two extreme possibilities and at least one of them is better than the other possible models.

Relative number of active nodes for each model can be determined directly from the $V.Q.$ of the shape of the unit cell in each model. The number of active nodes in various models with respect to that of TO model is depicted in Fig. 2.

Next, our goal is to determine the minimum transmission range needed for each model. Given a fixed sensing radius, r_s , the minimum required transmission ranges for the CB, *Alt-CB*, HP, *Alt-HP*, RD, and TO models are calculated below.

4.1.1. CB model

A cell has 26 neighboring cells: 6 *Type 1_{CB}* neighboring cells each shares whole one side of a cube, 12 *Type 2_{CB}* neighboring cells each shares a common line, and 8 *Type 3_{CB}* neighboring cells each shares just a common point with the cell (see Fig. 3).

The largest distance between any point in the cell and any point in a *Type 1_{CB}* neighboring cells is $r_s\sqrt{2}$; for *Type 2_{CB}* and *Type 3_{CB}* neighbors, it is $r_s\sqrt{3}$ and $2r_s$, respectively. The active node of a cell can communicate with active

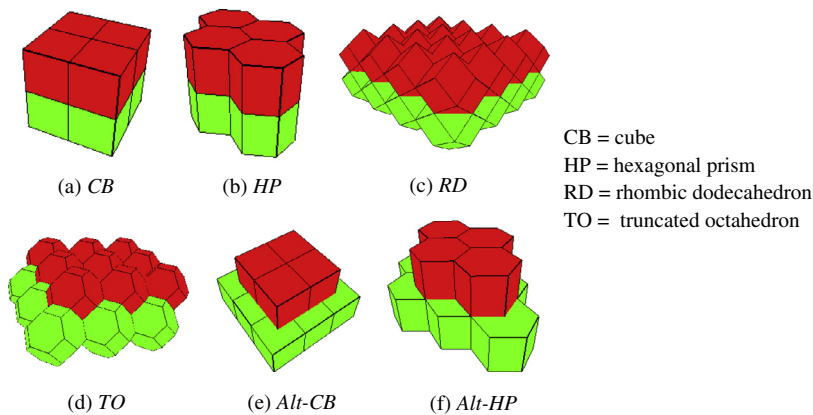


Fig. 1. Possible 3D space-partitioning shapes.

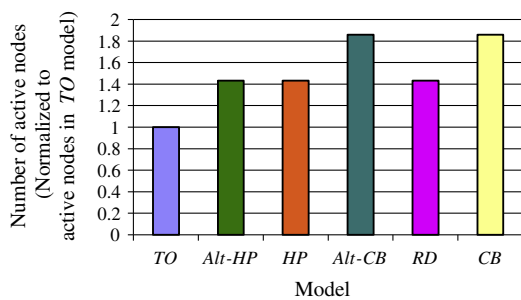


Fig. 2. The number of active nodes in various models.

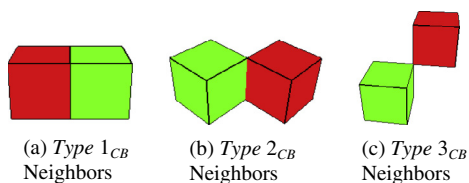


Fig. 3. Different types of neighbors in CB model.

nodes of all first-tier neighboring cells if the minimum transmission range is: $r_t = \max(r_s\sqrt{2}, r_s\sqrt{3}, 2r_s) = 2r_s$.

4.1.2. Alt-CB model

A cell has 16 first tier neighboring cells: 4 Type 1_{Alt-CB} neighboring cells each shares whole one side of a cube, 4 Type 2_{Alt-CB} neighboring cells each shares a common line, and 8 Type 3_{Alt-CB} neighboring cells each shares one quarter of one side of the cell (see Fig. 4).

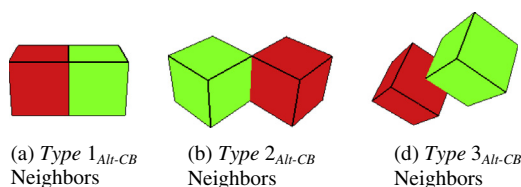


Fig. 4. Different types of neighbors in Alt-CB model.

The largest distance for Type 1_{Alt-CB}, Type 2_{Alt-CB} and Type 3_{Alt-CB} cells is $r_s\sqrt{2}$, $r_s\sqrt{3}$, and $r_s\sqrt{\frac{17}{6}}$, respectively. The minimum required transmission range in Alt-CB model is: $r_t = \max(r_s\sqrt{2}, r_s\sqrt{3}, r_s\sqrt{\frac{17}{6}}) = r_s\sqrt{3}$.

4.1.3. HP model

A cell has 20 first tier neighboring cells: 6 Type 1_{HP} neighboring cells each shares a common square plane, 2 Type 2_{HP} neighboring cells each shares a common hexagonal plane, and 12 Type 3_{HP} neighboring cells each shares a common line with the cell (see Fig. 5).

Suppose that each side of a hexagonal face of an HP cell is of length a , and its height is h . In an HP cell with optimal height, $h = a\sqrt{2}$. So the radius of the HP cell is $\frac{r_s}{2} = \sqrt{a^2 + (\frac{a^2}{2})} = a\sqrt{3}/\sqrt{2}$. Maximum distance from any point of the cell to any point of a Type 1_{HP}, Type 2_{HP}, and Type 3_{HP} neighbor is $\sqrt{(a\sqrt{13})^2 + h^2} = r_s\sqrt{\frac{5}{2}}$, $\sqrt{(2a)^2 + (2h)^2} = r_s\sqrt{2}$, and $\sqrt{(a\sqrt{13})^2 + (2h)^2} = r_s\sqrt{\frac{7}{2}}$, respectively. The active node of a cell can communicate with active nodes of all neighboring cells if the minimum transmission range is $r_t = \max(r_s\sqrt{\frac{5}{2}}, r_s\sqrt{2}, r_s\sqrt{\frac{7}{2}}) = r_s\sqrt{\frac{7}{2}}$.

4.1.4. Alt-HP model

A cell has 12 first-tier neighboring cells: 6 Type 1_{Alt-HP} neighboring cells each shares a square plane and 6 Type 2_{Alt-HP} neighboring cells each shares one third of a hexagonal plane with the cell (see Fig. 6).

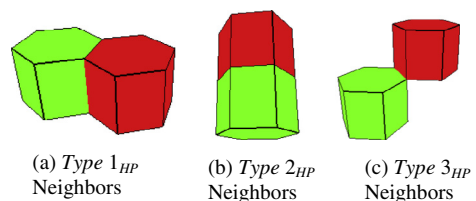


Fig. 5. Different types of neighbors in HP model.

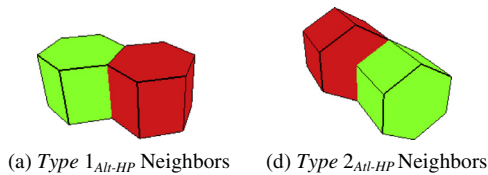


Fig. 6. Different types of neighbors in Alt-HP model.

Maximum distance for Type 1_{Alt-HP} and Type 2_{Alt-HP} neighbors is $\sqrt{(a\sqrt{13})^2 + h^2} = r_s\sqrt{\frac{5}{2}}$ and $\sqrt{(3a)^2 + (2h)^2} = r_s\sqrt{\frac{17}{6}}$, respectively. Thus the minimum transmission range needed is: $r_t = \max\left(r_s\sqrt{\frac{5}{2}}, r_s\sqrt{\frac{17}{6}}\right) = r_s\sqrt{\frac{17}{6}}$.

4.1.5. RD model

A cell has 18 first tier neighboring cells: 6 Type 1_{RD} neighboring cells each shares just a point and 12 Type 2_{RD} neighboring cells each shares a plane with the cell (see Fig. 7).

The maximum distance for Type 1_{RD} and Type 2_{RD} neighbor is $2r_s$ and $r_s\sqrt{\frac{5}{2}}$, respectively. Thus minimum transmission range required in RD model is: $r_t = \max\left(2r_s, r_s\sqrt{\frac{5}{2}}\right) = 2r_s$.

4.1.6. TO model

A cell has 14 first tier neighboring cells: 6 Type 1_{TO} neighboring cells each shares a common square plane and 8 Type 2_{TO} neighboring cells each shares a common hexagonal plane with the cell (see Fig. 8).

Maximum distance for Type 1_{TO} and Type 2_{TO} neighbor is $r_s\sqrt{17}/\sqrt{5}$ and $r_s\sqrt{14}/\sqrt{5}$, respectively. The active node of a cell can communicate with active nodes of all neighboring cells if the transmission range is at least: $r_t = \max\left(r_s\sqrt{\frac{17}{5}}, r_s\sqrt{\frac{14}{5}}\right) = r_s\sqrt{\frac{17}{5}}$.

The minimum transmission range required for maintaining connectivity in each model is shown in Fig. 9.

Next, we provide a comparison of the models based on energy consumption. We use a simplified model to calculate the network lifetime of the different partitioning schemes. We assume that the number of packets transmitted and relayed by a cell is the same in each model. Then, the lifetime of a cell depends on the transmission range used by a model and the number of nodes that resides inside a cell in that model. If we assume that the sensor

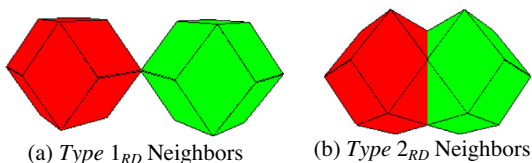


Fig. 7. Different types of neighbors in RD model.

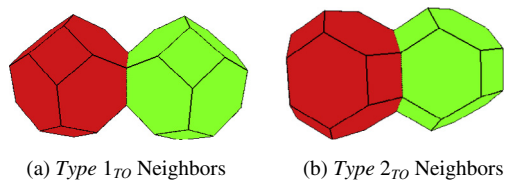


Fig. 8. Different types of neighbors in TO model.

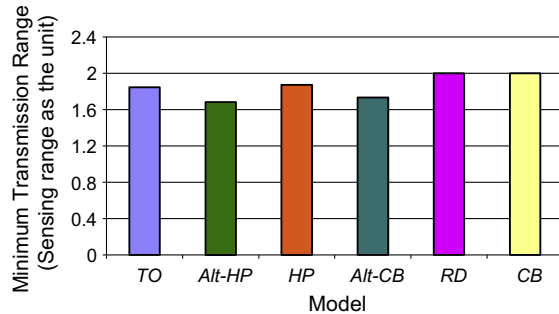


Fig. 9. Minimum transmission range required in different models.

nodes are uniformly distributed, the number of nodes in a cell is proportional to the volume of the cell. Finally, we assume that in our radio network, power consumption to transmit a packet is proportional to the square of the transmission range. Suppose that two models A and B has transmission range r_A and r_B , respectively. Volumes of a cell in models A and B are V^A and V^B , respectively. If cell lifetimes of models A and B are denoted by L^A and L^B , respectively, then we have:

$$\frac{L^A}{L^B} = \frac{r_B^2}{r_A^2} \times \frac{V^A}{V^B}$$

Using this equation, cell lifetime of each model, as compare to the cell lifetime of TO model, is calculated below:

$$\begin{aligned} \frac{L^{CB}}{L^{TO}} &= \frac{\left(r_s\sqrt{\frac{17}{5}}\right)^2}{(2r_s)^2} \times \frac{\frac{r_s^3}{3\sqrt{3}}}{\frac{4r_s^3}{5\sqrt{5}}} = \frac{17\sqrt{5}L^{Alt-CB}}{48\sqrt{3}L^{TO}} = \frac{\left(r_s\sqrt{\frac{17}{5}}\right)^2}{\left(r_s\sqrt{3}\right)^2} \times \frac{\frac{r_s^3}{3\sqrt{3}}}{\frac{4r_s^3}{5\sqrt{5}}} \\ &= \frac{17\sqrt{5}L^{HP}}{36\sqrt{3}L^{TO}} = \frac{\left(r_s\sqrt{\frac{17}{5}}\right)^2}{\left(r_s\sqrt{\frac{7}{2}}\right)^2} \times \frac{\frac{r_s^3}{4}}{\frac{4r_s^3}{5\sqrt{5}}} = \frac{17\sqrt{5}L^{Alt-HP}}{56L^{TO}} \\ &= \frac{\left(r_s\sqrt{\frac{17}{5}}\right)^2}{\left(r_s\sqrt{\frac{17}{6}}\right)^2} \times \frac{\frac{r_s^3}{4}}{\frac{4r_s^3}{5\sqrt{5}}} = \frac{3\sqrt{5}L^{RD}}{8L^{TO}} = \frac{\left(r_s\sqrt{\frac{17}{5}}\right)^2}{(2r_s)^2} \times \frac{\frac{r_s^3}{4}}{\frac{4r_s^3}{5\sqrt{5}}} = \frac{17\sqrt{5}}{64} \end{aligned}$$

The cell lifetimes of various models as compared to the cell lifetime of the TO model are shown in Fig. 10.

4.2. A distributed and scalable way for partitioning the volume

In order to select the subset of active nodes, first we need to find a scheme that allows each node to determine its cell in a distributed and scalable way. If every node knows which cell it belongs to, then choosing the active

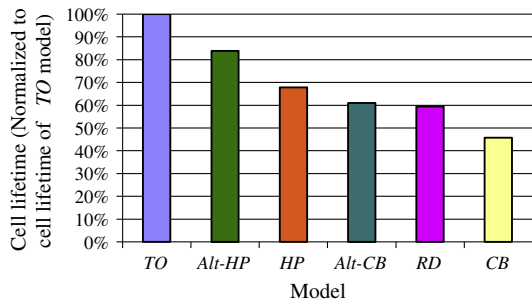


Fig. 10. Cell lifetime in various models.

node is easy, because all nodes that belong to a cell are within the transmission range of each other. A technique that allows every node to determine which cell it belongs to in a distributed and scalable way is described below. Since the technique is similar for all models, without loss of generality, we assume that the model is the *TO* model. We use the triple (u, v, w) as a unique cell id, and the cell which contains the information sink (*IS*) as having the cell id of $(0, 0, 0)$. If the coordinates of the *IS* are (x, y, z) , then the coordinates of the center of a virtual cell (u, v, w) can be expressed by the general equation as: $f(u, v, w) = \left(x + \frac{(2u+w)r_s}{\sqrt{5}}, y + \frac{(2v+w)r_s}{\sqrt{5}}, z + \frac{wr_s}{\sqrt{5}}\right)$. For example, a cell with id $(-1, -1, 2)$ has its center at coordinates $\left(x, y, z + \frac{2r_s}{\sqrt{5}}\right)$.

We assume that the sensing range r_s is embedded in the sensors before deployment. The *IS* broadcasts its coordinate (x, y, z) to all nodes, and a sensor node determines its own coordinate (x_s, y_s, z_s) using a localization scheme. In order to determine its cell id (u_s, v_s, w_s) , a brute force method is to check all possible values of (u_s, v_s, w_s) and choose the cell whose center has minimum Euclidean distance from the node, i.e.,

$$(u_s, v_s, w_s) = \arg \min_{u, v, w \in \mathbb{Z}} \left[\left(x_s - x - (2u + w) \frac{r_s}{\sqrt{5}} \right)^2 + \left(y_s - y - (2v + w) \frac{r_s}{\sqrt{5}} \right)^2 + \left(z_s - z - w \frac{r_s}{\sqrt{5}} \right)^2 \right],$$

where \mathbb{Z} is set of all integers. However, such an exhaustive search can easily be avoided. Since the value of a square term is never negative, we can set the value of the square terms to zero to get the values of u_s , v_s , and w_s . Since these values must be integer, we can get two possible integral values for each variable by taking ceiling (denoted by subscript h) and floor (subscript l):

$$\begin{aligned} u_l &= \left\lfloor \frac{(x_s - x - z_s + z)\sqrt{5}/2r_s}{1} \right\rfloor, & u_h &= \left\lceil \frac{(x_s - x - z_s + z)\sqrt{5}/2r_s}{1} \right\rceil, \\ v_l &= \left\lfloor \frac{(y_s - y - z_s + z)\sqrt{5}/2r_s}{1} \right\rfloor, & v_h &= \left\lceil \frac{(y_s - y - z_s + z)\sqrt{5}/2r_s}{1} \right\rceil, \\ w_l &= \left\lfloor \frac{(z_s - z)\sqrt{5}/r_s}{1} \right\rfloor, & w_h &= \left\lceil \frac{(z_s - z)\sqrt{5}/r_s}{1} \right\rceil. \end{aligned}$$

Thus we have eight possible values of (u_s, v_s, w_s) . Each node has to calculate its distance from each of the eight centers and choose the minimum one as its cell id; i.e.,

$$(u_s, v_s, w_s) = \arg \min_{\substack{u \in \{u_l, u_h\} \\ v \in \{v_l, v_h\} \\ w \in \{w_l, w_h\}}} \left[\left(x_s - x - (2u + w) \frac{r_s}{\sqrt{5}} \right)^2 + \left(y_s - y - (2v + w) \frac{r_s}{\sqrt{5}} \right)^2 + \left(z_s - z - w \frac{r_s}{\sqrt{5}} \right)^2 \right] \quad (1)$$

As cell id is a straightforward function of the location of a sensor, if a sensor knows its location, it can readily calculate its cell id. Once sensors have their cell id, then sensors with the same cell id can use any standard leader selection algorithms [24] to choose a leader among them, which can act as the active node of that cell. All nodes that have the same cell id are within the communication range of each other and the mechanism of keeping one node active among all the sensors with the same cell id is essentially same for both 2D and 3D networks. Thus results from 2D networks can be used here to achieve this goal.

4.3. *k*-coverage and performance analysis

While our approach of dividing a network into cells and keeping one node active in each cell allows us to achieve our goal in a highly distributed and scalable way, it does not always use minimum number of active nodes. The reason is obvious; since the active node is selected locally by the nodes inside a cell, it cannot compete with a centralized approach that has global information. However, it is important to evaluate how much efficiency is lost in our distributed scheme, comparing to such a centralized approach. To achieve this, we compare our scheme with the scheme where nodes can be placed at any desired location (as opposed to our random deployment), with an “oracle” deciding where to deploy those nodes. We call this comparison scheme *SuperOpt*.

A similar scheme in 2D that uses hexagonal shaped cells requires 4 times more nodes than *SuperOpt*. In the worst case, our scheme requires 8 times more nodes than *SuperOpt*. While this is not surprising, we find that it is possible to devise a similar highly distributed and scalable scheme in 3D that requires significantly fewer nodes for *k*-coverage with high probability. In what follows, we examine such a scheme.

4.3.1. *k*-coverage in 2D

Let us first explore how we can ensure *k*-coverage in 2D. For 1-coverage, we have to keep one node active in a hexagonal cell with radius $r = r_s/2$, where r_s is the sensing range of each sensor. A naïve approach, can simply keep *k* such node active in each cell. In that case, node requirement is still 4 times of the *SuperOpt* scheme. An alternative scheme would be to use smaller cells, while still keeping one node active in each cell. We determine that the radius of each cell has to be $r = r_s / \left(2\sqrt{\lceil k/4 \rceil}\right)$ in that case. This scheme provides *k*-coverage with high probability, but not with certainty when $k > 1$. We want to answer the following two questions:

1. What is the probability that this scheme has k -coverage?
2. How many nodes this scheme needs compare to *SuperOpt*?

To answer the two questions, first we need the help of the following theorem.

Theorem 4.1. *Suppose that we have two areas and in each area nodes are randomly distributed based on a 2D Poisson distribution. Then the sum of the number of nodes in two (independently) selected sub-areas is Poisson with parameter equal to the sum of the expected number of nodes in each individual area.*

Proof. Omitted due to space limitations.

Now, for our proposed scheme for 2D k -coverage, the area of each cell is $3\sqrt{3}r^2/2 = 3\sqrt{3}r_s^2/8\lceil k/4 \rceil$. Since we keep one node active in each such cell, active node density is $\rho = 1/\frac{3\sqrt{3}}{2} \frac{r_s^2}{4\lceil k/4 \rceil}$ node per unit area. Within r_s distance of any point, the number of active nodes is a *Poisson* random variable K with parameter: $\lambda_k = \frac{\pi r_s^2}{\frac{3\sqrt{3}}{2} \frac{r_s^2}{4\lceil k/4 \rceil}} = \frac{8\pi\lceil k/4 \rceil}{3\sqrt{3}}$. The probability that any point is within the sensing radius of at least k nodes is:

$$P(K \geq k) = 1 - P(K < k) = 1 - \sum_{i=0}^{k-1} P(K = i) \\ = 1 - \sum_{i=0}^{k-1} e^{-\lambda_k} \frac{\lambda_k^i}{i!} = 1 - e^{-\left(\frac{8\pi k/4}{3\sqrt{3}}\right)} \sum_{i=0}^{k-1} \left(\frac{8\pi k/4}{3\sqrt{3}}\right)^i / i!$$

Now, it can be shown that *SuperOpt* solution for k -coverage is dividing the 2D plane into hexagonal cells of radius r_s and keep k nodes active at the center of each cell. (Note that this scheme is not applicable when nodes are randomly deployed, we mention it here only to find a lower bound on the number of nodes needed for k -coverage). Thus the number of nodes needed by our proposed scheme is at most $\frac{3\sqrt{3}r_s^2/2k}{3\sqrt{3}r_s^2/8\lceil k/4 \rceil} = \frac{4\lceil k/4 \rceil}{k}$ times the number of nodes needed by *SuperOpt*.

From Table 1, we see that our proposed scheme provides 1-coverage with probability 1, but the active node requirement is 4 times than the lower bound. On the other hand, 4-coverage requires the same number of node as that of the lower bound, but the probability of at least k -coverage falls to 0.72. Note that *SuperOpt* assumes nodes can be deployed at any desired place, so the actual lower bound is likely larger, which in turn means that our scheme performs better than the above comparison. □

Table 1
Probability of k -coverage and node requirement in 2D.

K	λ_k	$P(K \geq k)$	Number of nodes vs. <i>SuperOpt</i> (%)
1	4.8367983	1	400
2	4.8367983	0.9616325	200
3	4.8367983	0.8688446	133
4	4.8367983	0.7192460	100
5	9.6735966	0.9639949	160

4.3.2. k -coverage in 3D

For 1-coverage, we have to keep one node active in a truncated octahedron cell with $r = r_s/2$, where r_s is sensing range of each sensor. For k -coverage, we propose the following scheme: set the radius of each truncated octahedron cell to $r = r_s/2\sqrt[3]{\lceil k/8 \rceil}$ and keep one node active in each cell. Then the volume of each cell is $32r^3/5\sqrt{5} = 4r_s^3/(5\sqrt{5}\lceil k/8 \rceil)$. Since we keep one node active in each such cell, active node density is $\rho = 5\sqrt{5}\lceil k/8 \rceil/(4r_s^3)$ node per unit volume. Within r_s distance of any point, the number of active nodes is a *Poisson* random variable K with parameter: $\lambda_k = \frac{4\pi r_s^3}{\frac{4}{5\sqrt{5}k/8}} = \frac{5\sqrt{5}\pi k/8}{3}$.

The probability that any point is within the sensing radius of at least k nodes is then given by:

$$P(K \geq k) = 1 - P(K < k) = 1 - \sum_{i=0}^{k-1} P(K = i) \\ = 1 - \sum_{i=0}^{k-1} e^{-\lambda_k} \frac{\lambda_k^i}{i!} = 1 - e^{-\left(\frac{5\sqrt{5}\pi k/8}{3}\right)} \sum_{i=0}^{k-1} \left(\frac{5\sqrt{5}\pi k/8}{3}\right)^i / i!$$

Now, it can be shown that one optimal solution for k -coverage is dividing the 3D space into hexagonal cells of radius r_s and keeping k nodes active at the center of each cell. (Note that this scheme is not applicable when nodes are randomly deployed, we mention it here only to find a lower bound on the number of nodes needed for k -coverage.) So the number of nodes needed by our proposed scheme is at most $\frac{\frac{32}{5\sqrt{5}} \frac{r_s^3}{k}}{\frac{32}{5\sqrt{5}k/8}} = \frac{8\lceil k/8 \rceil}{k}$ times the number of nodes needed by *SuperOpt* in 3D.

From Table 2, we see that our scheme achieves 4-coverage with probability 0.9971 with twice the number of nodes needed in *SuperOpt*. Unlike in 2D, we can achieve k -coverage with very high probability for higher values of k in 3D. Thus, the proposed scheme performs better in 3D than in 2D for larger values of k .

5. Discussions

Based on a number of assumptions, this paper provides the node placement strategy that achieves full coverage and connectivity for random node placement. The assumptions underlying our work, the sphere-based sensing, the sphere-based communication (disk based in 2D), and the homogenous sensing and communication range of each sensor, are standard assumptions in most network modeling works, and are applicable to the underwater

Table 2
Probability of k -coverage and node requirement in 3D.

K	λ_k	$P(K \geq k)$	Number of nodes vs. <i>SuperOpt</i> (%)
1	11.70802455	1	800
2	11.70802455	0.9999	400
3	11.70802455	0.9994	233
4	11.70802455	0.9971	200

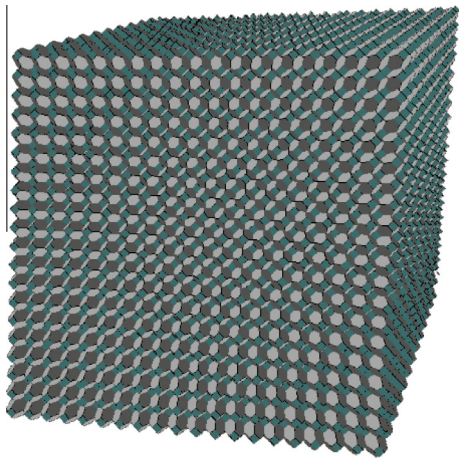


Fig. 11. Coverage of a cube shape 3D space in TO model with $20 \times 20 \times 20$ nodes.

networks as well. To adjust to real world situation, the network designer should conservatively estimate the sensing range and communication range (i.e., set sensing range and communication range at some fractional level of the actual sensing and communication range).

Our assumption of no boundary effect cannot be valid in practice, as of course all real networks will be finite in size. However, if the height, width and length of the network are sufficiently large as compared with the sensing range of each node, then a 3D volume of any shape can be covered with small overhead near the boundary. The smaller the sensing range, the smaller the boundary effect, with the boundary effect vanishes when the sensing range become infinitesimally small. Fig. 11 shows how a cube-shaped space is covered by a network consisting of $20 \times 20 \times 20$ nodes placed with the TO model.

Finally, our work does not require absolute positioning mechanism; rather any relative positioning mechanism where a node knows its position relative to the information sink or seed node is sufficient. Since in many sensor network applications (e.g., detection, monitoring) it is important to know from where information originates, sensor networks that are deployed for such application must already include some positioning mechanism. Thus, our node placement strategy can get the position information from such a mechanism without adding any extra expense.

Our focus in this paper was on the relationship between connectivity and coverage in 3D networks. Of course, this is just “one piece of the puzzle” which relates to many other aspects of design, implementation, and operation of a 3D underwater networks. As an example, we did not discuss here routing in such a 3D network; neither the route establishment process, nor the relationship between connectivity and the route determination. We also did not discuss the management of the sleep-wake patterns and the related required coordination. Furthermore, there are other technologies that are of fundamental importance to enable the schemes presented here, such as underwater localization (e.g., [44–46]), for instance.

6. Conclusions

In this paper, we investigate the coverage and connectivity issues in three-dimensional networks in situations where it is difficult to deploy and maintain nodes in pre-determined positions. As a result, a large number of nodes has to be randomly and uniformly deployed, such that full sensing coverage can still be achieved. However, at any time instant not all nodes are required for full sensing coverage. It is important to dynamically put those redundant nodes into sleep mode to increase network lifetime. We provide a highly distributed and scalable scheme to achieve this goal in 3D networks. While an analogous solution exists for 2D networks, transition from 2D to 3D is typically a difficult task, given that many problems in 3D are harder than their 2D counterparts by orders of magnitude. In order to make the solution highly distributed and scalable, we partition the 3D network space into identical regions (or, cells) and keep one node active in each such cell. Finding the right partitioning scheme for 3D networks – one of the most challenging problems of this work – is also the main contribution of this paper. Using a century-old Kelvin’s conjecture, we show that truncated octahedral tessellation of 3D space is the most plausible solution for this problem. We define a metric called volumetric quotient (*V.Q.*) that is a measure of the quality of the competing space-filling polyhedrons for our problem. The higher the *V.Q.* of the shape of a cell, the lower the number of active nodes required for full coverage. Truncated octahedron turns out to be the best choice with *V.Q.* of 0.68329, which is much better than the *V.Q.* of the other possible choices (both optimized hexagonal prism and rhombic dodecahedron have *V.Q.* of 0.477, while cube has just 0.36755). We also compared different partitioning schemes based on their energy consumption, and we found that the truncated octahedron based partitioning scheme has longer cell lifetime than the other schemes. We describe a mechanism for each sensor node to determine which cell it belongs to based on the cell’s own position, by using a simple set of arithmetic operations. No message passing between nodes in different cells is needed to choose the active nodes. We extend our work for *k*-coverage, where sensing coverage by *k* sensor nodes is needed. Our scheme can provide *k*-coverage in 3D with high probability, while significantly decreasing the gap with the centralized scheme with respect to the number of active nodes required. While the relative number of active nodes can be decreased in both 2D and 3D, the *k*-coverage in 3D can be ensured with high probability.

Acknowledgements

This work was supported in part by the US National Science Foundation Grant Nos. ANI-0329905, CNS-0626751, CNS-1040689, and ECCS-1308208 and by the US Air Force Office of Scientific Research under contract number FA9550-09-1-0121/Z806001.

References

- [1] I.F. Akyildiz, D. Pompili, T. Melodia, Underwater acoustic sensor networks: research challenges, *Ad Hoc Netw. J.* (2005).
- [2] S.M.N. Alam, Z.J. Haas, Coverage and connectivity in three-dimensional networks, in: *Proceedings of ACM MobiCom*, 2006.
- [3] S.M.N. Alam, Z. Haas, Coverage and connectivity in three-dimensional underwater sensor networks, *Wirel. Commun. Mob. Comput.* 8 (2008) 995–1009.
- [4] Aristotle, *On the Heaven*, vol. 3, 350BC (chapter 8).
- [5] X. Bai, S. Kumar, Z. Yun, D. Xuan, T.H. Lai, Deploying wireless sensors to achieve both coverage and connectivity, in: *Proceedings of ACM MobiHoc*, 2006.
- [6] E.S. Barnes, N.J.A. Sloane, The optimal lattice quantizer in three dimensions, *SIAM J. Algebr. Discrete Meth.* 4 (1983) 30–41.
- [7] S. Basagni, A. Carosi, C. Petrioli, Sensor DMAC: dynamic topology control for wireless sensor networks, in: *IEEE VTC*, 2004.
- [8] J. Carle, J.F. Myoupo, D. Semé, A basis for 3-D cellular networks, in: *Proceedings of the 15th International Conference on Information Networking*, 2001.
- [9] K. Chakrabarty, S.S. Iyengar, H. Qi, E. Cho, Grid coverage for surveillance and target location in distributed sensor networks, *IEEE Trans. Comput.* 51 (12) (2002) 1448–1453.
- [10] B. Chen, K. Jamieson, H. Balakrishnan, R. Morris, Span: an energy-efficient coordination algorithm for topology maintenance in ad hoc wireless networks, *Wireless Netw.* 8 (5) (2002).
- [11] W. Cheng, A.Y. Teymorian, L. Ma, X. Cheng, X. Lu, Z. Lu, Underwater localization in sparse 3D acoustic sensor networks, in: *INFOCOM*, 2008, pp. 236–240.
- [12] T. Couqueur, V. Phipatanasuphorn, P. Ramanathan, K.K. Saluja, Sensor deployment strategy for target detection, in: *Proceeding of the First ACM International Workshop on Wireless Sensor Networks and Applications*, 2002, pp. 169–177.
- [13] S. Datta, T. Woody, Go Green, Get Rich: 8 Technologies to Save the World, *Business 2.0 Magazine*, January 2007 <<http://money.cnn.com/galleries/2007/biz2/0701/gallery.8greentechs/2.html>>.
- [14] C. Decayeux, D. Semé, A new model for 3-D cellular mobile networks, in: *ISPD/HeteroPar*, 2004.
- [15] S. Durocher, D. Kirkpatrick, L. Narayanan, On routing with guaranteed delivery in three-dimensional ad hoc wireless networks, in: *ICDCN*, 2008.
- [16] M. Gardner, *The Sixth Book of Mathematical Games from Scientific American Chicago*, University of Chicago Press, IL, 1984.
- [17] T.C. Hales, A proof of the Kepler conjecture, *Ann. Math.* 162 (2005) 1065–1185.
- [18] D. Hilbert, S. Cohn-Vossen, *Geometry and the Imagination*, Chelsea, New York, 1999.
- [19] J. Heidemann, W. Ye, J. Wills, A. Syed, Y. Li, Research challenges and applications for underwater sensor networking, in: *Proceedings of the IEEE Wireless Communications and Networking Conference*, IEEE, Las Vegas, Nevada, USA, 2006.
- [20] N.W. Johnson, *Uniform Polytopes*, Cambridge University Press, Cambridge, England, 2000.
- [21] R. Kershner, The number of circles covering a set, *Am. J. Math.* 61 (1939) 665–671.
- [22] M. Křížek, Super convergence phenomena on three-dimensional meshes, *Int. J. Numer. Anal. Model.* 2 (1) (2005) 43–56.
- [23] D. Li, K. Wong, Y.H. Hu, A. Sayeed, Detection, classification and tracking of targets in distributed sensor networks, *IEEE Signal Process. Magaz.* 19 (2) (2002).
- [24] N. Lynch, *Distributed Algorithms*, Morgan Kaufman Publishers, Wonderland, 1996.
- [25] S. Meguerdichian, F. Koushanfar, M. Potkonjak, M.B. Srivastava, Coverage problems in wireless ad-hoc sensor networks, in: *INFOCOM'01*, 2001, pp. 1380–1387.
- [26] H. Steinhaus, *Mathematical Snapshots*, third ed., Oxford University Press, 1969.
- [27] W. Thomson, (Lord Kelvin), On the division of space with minimum partition area, *Philos. Magaz.* 24 (1887) 503–514. <http://zapatopi.net/kelvin/papers/on_the_division_of_space.html>.
- [28] P. Varshney, *Distributed Detection and Data Fusion*, Springer-Verlag, New York, NY, 1996.
- [29] D. Weaire, *The Kelvin Problem: Foam Structures of Minimal Surface Area*, Taylor and Francis, London, 1996.
- [30] D. Weaire, R. Phelan, A counter-example to Kelvin's conjecture on minimal surfaces, *Philos. Magaz. Lett.* 69 (1994) 107–110.
- [31] D. Wells, *The Penguin Dictionary of Curious and Interesting Geometry*, Penguin, London, 1991.
- [32] H. Weyl, *Symmetry*, Princeton University Press, Princeton, NJ, 1952.
- [33] G. Xing, X. Wang, Y. Zhang, C. Lu, R. Pless, C.D. Gill, Integrated coverage and connectivity configuration for energy conservation in sensor networks, in: *TOSN*, vol. 1(1), 2005.
- [34] Y. Xu, J. Heideman, D. Estrin, Geography-informed energy conservation in ad hoc routing, in: *Proceedings of the 7th ACM MobiCom*, July 2001.
- [35] F. Ye, G. Zhong, S. Lu, L. Zhang, PEAS: a robust energy conserving protocol for long-lived sensor networks, in: *ICDCS '03*, Rhode Island, 2003.
- [36] M. Younis, K. Akkaya, Strategies and techniques for node placement in wireless sensor networks: a survey, *Ad Hoc Netw.* 6 (2008) 621–655.
- [37] H. Zhang, J.C. Hou, Maintaining sensing coverage and connectivity in large sensor networks, *Wirel. Ad Hoc Sensor Netw.: An Int. J.* 1 (1–2) (2005) 89–124.
- [38] K. Ovaliadis, N. Savage, V. Kanakaris, Energy efficiency in underwater sensor networks: a research review, *J. Eng. Sci. Technol. Rev.* 3 (1) (2010) 151–156.
- [39] T. Melodia, H. Kulhandjian, L.-C. Kuo, E. Demirors, Advances in underwater acoustic networking, in: *Mobile Ad Hoc Networking, Cutting Edge Directions*, second ed., Wiley Online Library, 2013, March 4 (Chapter 23).
- [40] P. Pandey, D. Pompili, Distributed computing framework for underwater acoustic sensor networks, in: *2013 IEEE International Conference on Distributed Computing in Sensor Systems*, May 20–23, 2013.
- [41] S. Ibrahim, M. Al-Bzoor, J. Liu, R. Ammar, J.-H. Cui, S. Rajasekaran, General optimization framework for surface gateway deployment problem in underwater sensor networks, *EURASIP J. Wirel. Commun. Network.* 2013 (2013) 128.
- [42] Richard Fitzpatrick, "Euclid's Elements of Geometry," the Greek text of J.L. Heiberg (1883–1885) from "Euclid's Elementa, edidit et Latine interpretatus est I.L. Heiberg, in: aedibus B.G. Teubneri, 1883–1885," Richard Fitzpatrick, December 2007.
- [43] F. Senel, K. Akkaya, T. Yilmaz, Autonomous deployment of sensors for maximized coverage and guaranteed connectivity in underwater acoustic sensor networks, in: *IEEE LCN'13*, 2013, pp. 211–218.
- [44] Z. Zhou, J.-H. Cui, S. Zhou, Efficient localization for large-scale underwater sensor networks, *Ad Hoc Netw.* 8 (3) (2010) 26–279.
- [45] M. Erol-Kantarci, S. Oktug, L. Vieira, M. Gerla, Performance evaluation of distributed localization techniques for mobile underwater acoustic sensor networks, *Ad Hoc Netw.* 9 (1) (2011) 6–72.
- [46] K.-C. Lee, J.-S. Ou, M.-C. Huang, Underwater acoustic localization by principal components analyses based probabilistic approach, *Appl. Acoust.* 70 (9) (2009) 116–1174.



S.M. Nazrul Alam received his Ph.D. in Computer Science from Cornell University in 2010. Before that he received his M.Sc. in Computer Science from University of Toronto. He is a recipient of University Gold Medal and Sharfuddin Gold Medal from Bangladesh University of Engineering and Technology for outstanding academic performance during his undergraduate studies. After completion of his graduate studies, Nazrul joined a startup working on business analytics. Subsequently, he moved to Mountain View, California for his

new adventure at Google where he is currently working on identity and authentication. His research interests include wireless networks, three-dimensional networks, online security and privacy.



Zygmunt J. Haas received his Ph.D. in 1988 from Stanford University in Electrical and Computer Engineering. In 1988, he joined the AT& T Bell Laboratories in the Network Research Area. There he pursued research in wireless communications, mobility management, fast protocols, optical networks, and optical switching. In August 1995, he joined the faculty of the School of Electrical and Computer Engineering at Cornell University, where he is now a Professor. He heads the Wireless Network Laboratory (wnl.ece.cornell.edu), a research group with extensive contributions and international recognition in the area of Ad Hoc Networks and Sensor Networks. Dr. Haas is an IEEE Fellow and an author of over 200 technical conference and journal papers and holds eighteen patents in the areas of wireless

networks and wireless communications, optical switching and optical networks, and high-speed networking protocols. He won a number of awards and distinctions, including “Best Paper” awards and the 2012 IEEE ComSoc WTC Recognition Award for “outstanding achievements and contribution in the area of wireless communications systems and networks”. Dr. Haas chaired and co-chaired several key conferences in the communications and networking areas, organized many workshops, delivered numerous tutorials at major IEEE and ACM conferences, and served as an IEEE ComSoc Distinguished Lecturer. He has been editor of many journals and magazines, including the IEEE Transactions on Networking, the IEEE Transactions on Wireless Communications, the IEEE Communications Magazine, and the Springer Wireless Networks journal (WINET). His interests comprise: mobile and wireless communication and networks, modeling and performance evaluation of large and complex systems, and biologically-inspired networks.

Please cite this article in press as: S.M. Nazrul Alam, Z.J. Haas, Coverage and connectivity in three-dimensional networks with random node deployment, Ad Hoc Netw. (2014), <http://dx.doi.org/10.1016/j.adhoc.2014.09.008>